International Journal of Applied Engineering Research ISSN 0973-4562 Volume 10, Number 23 (2015) pp 43492-43500

Optimal Location and Performance Analysis of IPFC Using Adaptive Differential Evolution

Dr. S. Arul

Associate Professor, Department of Electronics and Communication Engineering, Jeppiaar Institute of Technology, Chennai, India. Email: s_arul75@yahoo.co.in

Abstract

This paper presents a new approach for determinations of optimal locations of interline power flow controller (IPFC) using adaptive differential evolution (ADE) under multiline transmission. The main objective is to reduce real power loss, overloading of the lines and bus voltage limit violation. An objective function is formulated for the above objectives and a mathematical model is derived for the objective function. An adaptive proportional integral controller (APIC) is developed for controlling real and reactive power flow. Sensitivity analysis is used to estimate the optimal location of buses. The simulation is carry out using MATLAB for two test cases using an IEEE 30-bus and IEEE 57-bus test system. Simulation results indicate that the location and parameters optimized by using ADE minimizing overloaded lines, bus voltage abuse and congestion management. Simulation results obtained for both the IEEE 30-bus and IEEE 57-bus using proposed method is compared with particle swarm optimization (PSO). The obtained results show that the ADE technique provides good computational efficiency, less cost of congestion removal, low power loss, fast and stable convergence characteristics.

Keywords: IPFC, Sensitivity analysis, adaptive differential evolution, overloading, objective function, adaptive PI controller

1. Introduction

There is a huge increase in the power transactions due to power system reformation and various factors such as environmental, high cost, etc. are major hurdles for power transmission system. Flexible AC Transmission Systems (FACTs) devices are introduced to increase power transfer capability, reduce system losses and stability. To change power flow in the lines Unified power flow controller (UPFC) and IPFC can be used by changing their parameters. FACT devices can control the system parameters dynamically thus controlling of steady state power flow [1, 2]. The network power flow can be controlled by introducing FACT devices by estimating the exact location without affecting the work schedule and topology of the network [3]. UPFC can be incorporated directly for bus and line voltage control, phase shifter, series compensation, etc. UPFC has the property of both the series and shunt controller and it has better control over one-converter FACTs controller. UPFC is one of the promising FACT controllers for selectively control the active or reactive power flow on the line [4, 5].

IPFC combines two or more FACT controllers in series and can control power flows of a group of lines and sub-networks. On the other hand the UPFC can control power flow of single transmission line only. The IPFC also has the capability to directly transfer real power between compensated lines and transfer power demand from over loaded to under loaded lines [6, 7]. To solve power system state estimation problem Taguchi differential evolution algorithm is used. For improving the accuracy and reliability of state estimation problem the positive properties of Taguchi method is combined with the differential evolution [8]. Application of differential evolution algorithm for transient stability with different constrains to get optimal power flow has been introduced by Cai et al [9]. A modified differential evolution algorithm with fitness sharing for increasing the stability, reduce overload and voltage violations of power system [10].

An integral plus double derivative with two degree of freedom controller is proposed for automatic generation control. The controller gains and other parameters are optimized using an evolutionary computational technique. The system dynamic response is compared with PI (proportional integral) and PID (proportional integral and derivative) controller with two degree of freedom [11]. A new approach for reuse the code of Newton-Raphson is introduced in the power flow analysis of IPFC. Different practical transmission stations have been taken into account and the complexity of the program is studied [12]. A hybrid technique based optimal location finding and size estimation for improving the dynamic stability of the system is proposed by Vijay Kumar and Srikanth [13]. A particle swarm optimization (PSO)-based algorithm is used to estimate exact location and sizing of unified power flow controller to perform congestion management. The impact of load variations, system reliability and congestion cost of the system has been studied [14]. Automatic human motion tracking in video sequences using PSO technique is proposed by Sanjay et al [15]. Computer vision and pattern recognition is used to identify the motion of human and high search space is used for high variability in human appearance.

In this paper, a new optimization algorithm is introduced for determining the optimal location thereby bus voltage limit violation, overloading of lines and congestion management can be done. The voltage limit violations, overloading of line can be eliminated or reduced by using the proposed technique. The performance of the proposed system is compared with other optimization techniques such as PSO and GA. The remainder of this paper is organized as follows: section 2 describes the Mathematical Model of IPFC; section 3 describes problem formulation with objective function;

section 4 explains the proposed adaptive differential evolution algorithm; section 5 explains the simulation results and discussion; and finally, conclusion is discussed in section 6.

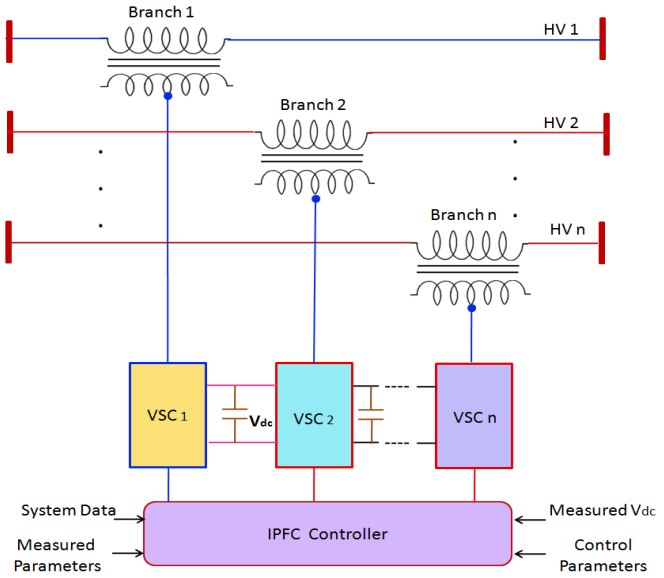

Fig. 1. Schematic diagram of two converter model of IPFC.

2. Mathematical Model of IPFC

The issues and related problems for optimal power flow and integration of FACT devices has been reported in [20, 21]. In this paper, controlling of real and reactive power flow, regulating bus voltage and congestion management of IPFC has been studied. The IPFC consists of number of solid-state voltage sources converters (VSCs). Generally the simple IPFC has two back to back connected DC-AC converters which are in series with two transmission lines through transformers. A common DC link is used to connect the DC terminals of the converters. Fig.1 shows such arrangement of IPFC. The IPFC is incorporated between the line-1 where the bus A and B are connected and line-2 where bus B and C are connected. A mathematical model of IPFC based on power injection model and the π-equivalent circuit is shown in fig. 2.

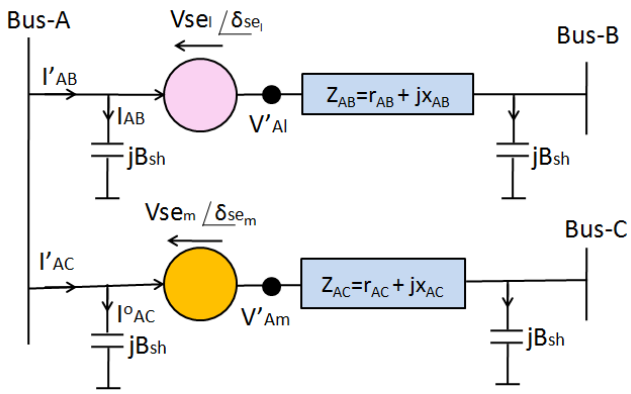

Fig. 2. Equivalent circuit of IPFC

The node X and Y are the dummy buses which connect the IPFC to the line 1 and 2 respectively. The complex bus voltages V_A, V_B and V_C for the buses A, B, C are defined as $V_A\angle\theta_A, V_B\angle\theta_B, V_C\angle\theta_C$ respectively. The active and reactive power injections at buses A, B, and C is shown in fig. 3. The mathematical equations can be derived for IPFC with any number of series converters. Line-1 and 2 of fig. 2, the relation between node current and voltage of the line can be derived. The mathematical equations based on the principle of IPFC can be given as:

$$V_B^{'} = V_A + V_{se_{AB}}, I_B^{'} = \frac{V_B^{'} - V_B}{Z_{AB}} \quad (1)$$

$$I_{AB}^{0} = \frac{jV_B B}{2}, I_{AB} = I_{AB}^{0} + I_{AB}^{'} \quad (1)$$

The power flow equations from bus A –B and bus B-A is written as

$$S_{AB}^{a} = P_{AB}^{a} + jQ_{AB}^{a} = V_A I_{AB}^{*} = V_A [I_{AB}^{0} + I_{AB}^{'}]^{*} \quad (2)$$

$$S_{AB}^{U} = P_{BC}^{a} + jQ_{BC}^{a} = V_B I_{BC}^{*} = V_B [I_{BC}^{0} + I_{BC}^{'}]^{*} \quad (2)$$

The power injection of line-1 and lin-2 can be derived according to the equivalent circuit of IPFC as:

$$P_{A1} = -V_a V_{se}[G_{in}\cos\delta_{Ase} + B_{in}\sin\delta_{Ase}] \quad (3)$$

$$P_{n1} = V_n V_{se}[G_{in}\cos\delta_{nse} + B_{in}\sin\delta_{nse}] \quad (4)$$

$$Q_{A1} = -V_a V_{se}[G_{in}\sin\delta_{Ase} - B_{in}\cos\delta_{Ase}] \quad (5)$$

$$Q_{n1} = V_n V_{se}[G_{in}\sin\delta_{Ase} - B_{in}\cos\delta_{Ase}] \quad (6)$$

Active and reactive power flows in the line-1 and line-2 having IPFC can be written, using (1) and (2) can be written as:

$$P_{in}^{1} = V_A^2 G_{An} - V_A V_n[G_{An}\cos\delta_{An} + B_{An}\sin\delta_{An}] + V_A V_{se}[G_{An}\cos(\delta_A - \delta_{se}) + B_{An}\sin(\delta_A - \delta_{se})] \quad (7)$$

$$Q_{in}^{1} = -V_A^2\left(B_{An} + \frac{B}{2}\right) - V_A V_n[G_{An}\sin\delta_{An} + B_{An}\cos\delta_{An}] + V_A V_{se}[G_{An}\sin(\delta_A - \delta_{se}) - B_{An}\cos(\delta_A - \delta_{se})] \quad (8)$$

$$P_{in}^{1} = V_A^2 G_{An} - V_A V_n[G_{An}\cos\delta_{An} - B_{An}\sin\delta_{An}] - V_A V_{se}[G_{An}\cos(\delta_A - \delta_{se}) + B_{An}\sin(\delta_A - \delta_{se})] \quad (9)$$

$$Q_{in}^{1} = -V_A^2\left(B_{An} + \frac{B}{2}\right) + V_A V_n[G_{An}\sin\delta_{An} + B_{An}\cos\delta_{An}] - V_A V_{se}[G_{An}\sin(\delta_A - \delta_{se}) - B_{An}\cos(\delta_A - \delta_{se})] \quad (10)$$

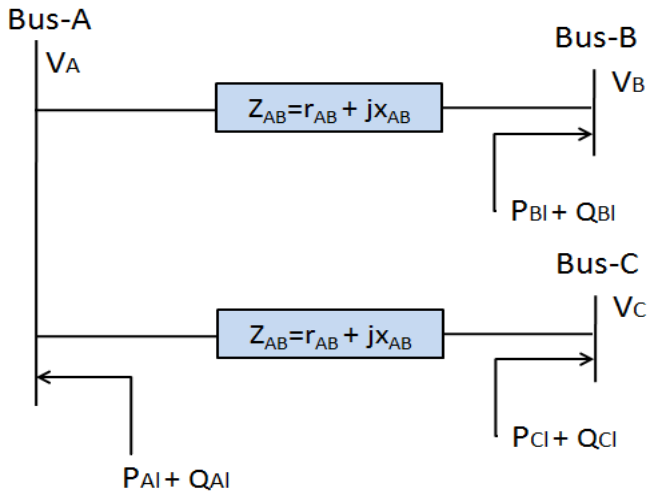

Fig. 3. Injection model of IPFC.

3. Problem Formulation

An IPFC is a flexible AC transmission system (FACTS) device which can be capable to compensate multiple lines simultaneously. Usually series capacitors are used to improve the transfer of real power but it cannot control the reactive power in a given line, this results to improper compensation. If capacitive combination is used, the ratio of reactance to resistance (X/R) is improper which leads to unbalance in the load. The IPFC has the capacity to control reactive series compensation of each line. So that it improves the real power transfer between the compensated lines. The basic diagram of IPFC is shown in fig. 1. The voltage-source converter (VSC) is injecting variable amplitude sinusoidal voltage and it is interfaced with a DC link. In order to maintain the load balancing of transmission line network, thyristor controlled capacitive compensation is being used for transferring active power [16]. The total active power transfer from VSC to transmission lines is equal to zero if losses are neglected.

A. Objective Function

The main aim of this work is to minimize overloaded line and eliminating the voltage violations present in the lines. The objective function for optimizing the power system is given as [17,18].

$$F=\sum_{i=1}^{Nl} w_i\left(\frac{A}{A_{max}}\right)^{2\lambda}+\sum_{m=1}^{Gb} w_i\left(\frac{V_{ref}-V_m}{V_{ref}}\right)^{2r} \quad (11)$$

Where Nl is the number of lines, w_i is the weighting factor, A is the current apparent power, A_{max} is the rate of current apparent power, Gb is the number of buses, V_m is the voltage magnitude at bus m, V_{ref} is the nominal voltage at bus m and the coefficients r and λ are used to penalize more or less over voltage and load violations.

B. Constraints

The main objective of this study is to determine the optimal location of IPFC for reducing the violations present in the power system. In this paper, IEEE 30-bus and IEEE 57-bus multiline outage contingencies are considered. A voltage limit violation present in the buses and overloaded lines are represented by the following constraints:

Voltage constraints: $V_L^{min} \le V_L \le V_L^{max}$; $L \in N_N$

Line flow limit: $F_L^{min} \le F_L \le F_L^{max}$; $L \in N_F$

Tap position constraints: $T_L^{min} \le T_L \le T_L^{max}$; $L \in N_T$

Power generation limit: $P_L^{min} \le P_L \le P_L^{max}$; $L \in N_P$

After estimating the critical emergency the ADE is applied for finding the optimal location and other parameters of IPFC. The severity order is allotted according to the violation limit. After inserting the IPFC in estimated location it will eliminate the bus voltage violation and minimize the overloading. The lower and upper bounded values of each generator can be represented as follows:

$$P_G^{min} \le P_G \le P_G^{max} \quad (12)$$

$$Q_G^{min} \le Q_G \le Q_G^{max} \quad (13)$$

Where P_G^{min} is the lower bound and P_G^{max} is the upper bound of real power of a specified generator and Q_G^{min} is lower band and Q_G^{max} is the upper bounds of reactive power of a specified generator respectively. In the same way the upper and lower voltage limits of each load bus is given by:

$$V^{min} \le V \le V^{max} \quad (14)$$

Where, V^{min} and V^{max} are the lower and upper voltage limits of a specified bus.

4. Adaptive Differential Evolution

Differential evolution (DE) is an optimization algorithm which was introduced by Storn and Price [19]. DE is a heuristic, population-based algorithm similar to evolutionary algorithms which utilize population of points for estimating global minimum of s function over continuous search space. There are several variants of DE and it can be expressed as:

$$DE/mv/df/cs \quad (15)$$

where mv, df and cs represents the mutated vector, number of difference vector and crossover scheme respectively. DE has three man advantages such as rapid convergence, ability to locate accurate global optimum values and use few control parameters for estimation. The procedure of DE is almost equal to PSO except cross over and mutation. It can also work with multi-dimensional, noisy and time dependent objective functions [20]. Based on these advantages, in this paper, we choose ADE for optimal location and parameter setting problem in IPFC. The step by step implementation of ADE is described as follows:

Step 1. The parameters of ADE such as size of population (SP), maximum number of iterations (I_{max}), power flow data, the variables to be optimized, F, and CR.

Step 2. The SP of D-dimensional parameter vector U_i^k and the population of solution P^k, $P_u^k = U_i^k$, i=1,2,...,NP; k=1,2,...,k_{max} and $U_i^k = U_{j,i}^k$, j=1,2,...,D.

The index, i represent the population index, j represents the parameters within the vectors and k is the generation to which a vector belongs.

The population NP has D-dimensional vectors $U_i^k = [U_{1,i}^k, U_{2,i}^k, \dots, U_{j,i}^k, \dots, U_{D,i}^k]$. Each vector forms a candidate solution to the D-dimensional optimization problem and values are randomly selected within the interval U_L and U_M. $U_L = [U_{1,L}, U_{2,L}, \dots, U_{D,L}]$ and $U_M = [U_{1,M}, U_{2,M}, \dots, U_{D,M}]$ are the lower and upper limits of the search space. Now the initial population in the search space by:

$$U_{j,i}^1 = U_L + rand[1](U_M - U_L) \quad (16)$$

The solution of parameter estimation is feasible because they are initialized within the feasible range and we have to find the optimal one.

step 2. according to (9) evaluate the fitness of each individual in the population.

step 3. create new population by:

(1) Mutation factor adaption: Each individuals U_i^k and associated individuals are mutated with the mutation rate M_r and obtained by the strategy DE/mu/dv/cr [21] as follows:

A trial vector V_i^k is created by adding the third vector to the difference between the two vectors and is given by

$$V_i^k = U_{r1}^k + F(U_{r2}^k - U_{r3}^k) \quad (17)$$

where F is the mutation scaling factor having range (0,1) and is given by

$$F_i^{k+1} = \begin{cases} 1 - rand_1^{\left(1-\frac{k}{k_{max}}\right)^b}, if\ rand_2 < M_r \\ F_i^k, otherwise \end{cases} \quad (18)$$

where k is the current generation, k_{max} is the maximum generation, and $rand_1$ and $rand_2$ are the uniform random values within the range [0,1]. The scaling factor F, should be adaptive with the following mutation rate M_r and is determined as:

$$M_r = \frac{f(U_i^k) - min(f(U_i^k))}{max(f(U_i^k)) - min(f(U_i^k))} \quad (19)$$

f(.) is the objective function.

(2) Crossover adaptation: The crossover rate RC_i is independently calculated for each vector as:

$$RC_i = rnd_i(P_{RC}^k, 0.1) \quad (20)$$

where P_{RC}^k is the mean value to generate RC_i. It is updated as:

$$P_{RC} = (1-q)P_{RC} + q\ mean_A(S_{RC}) \quad (21)$$

where q is a constant in the range (0,1), S_{RC} is the set of successful rate of RC_i and $mean_A(.)$ is the usual arithmetic mean operation.

(3) Selection: For each $U_{j,i}$ and corresponding $Y_{j,i}$ to select next generation vector, k=k+1 as:

$$U_i^{k+1} = \begin{cases} Y_i^k, if\ J(Y_i^k) < J(U_i^k) \\ U_i^k, otherwise \end{cases} \quad (22)$$

where J(U) is the objective function to be minimized. Thus, the new trial vector swaps its values with the target, if objective function value is less otherwise the target is conserved in the population.

5. Simulation results and discussion

The simulation was developed using matlab code and performed on matlab version 2013, Intel core i5, 2.3 GHz with 6GB RAM computer. To measure the real and reactive power flow of both the lines two different cases has been considered. In the first case IPFC is activated and the dynamic performance of both the PI and API has been simulated and compared with unit-step changes of the system. On the other hand, the R_L/X_L is increased three times than the first case and other parameters are same. The control system performance measurements, namely the integral absolute error (IAE) and the integral square error (ISE) have been calculated.

The performances of both the ADE and PSO algorithms are studied together for comparison. To study the performance of both the ADE and PSO the IEEE 30-bus and IEEE 57-bus test systems are used in this work. The network topology and data for simulating above systems are taken from [22, 23] respectively. Different initial parameters have been used for implementing ADE and PSO to find the optimal values of IPFC are presented in table 1. The parameter values for optimal calculation are adopted according to the literature [24-26]. The ADE and PSO techniques do not have standard values for their parameters because they are probable based techniques. So that the best adopted values stated in the literature [27, 28] are chosen and the result were evaluated statistically. In this paper, the performance of ADE and PSO for IEEE 30-bus and IEEE 57-bus system has been performed for 100 trials and the results are as follows:

Table 1. Initialization parameters for implementing ADE and PSO

ADE Technique		PSO Technique	
Population Size	50	Number of swam	50
Maximum number of generations	100	Maximum number of flights	100
Number of variables	3	w_{max}	0.9
Length of individuals	3	W_{min}	0.4
Step size	0.5	Termination criteria	1.exp-6
Crossover probability constant	0.5	c1, c2	0.9
Termination criteria	1.exp-6	Deviation	10

A. IEEE 30-bus System

This system consists of 30 buses, 42 transmission lines, 15 loads, and 5 generators with seven possible contingencies. The base voltage (line-to-line) is 160 kV and power is 100 MVA. The generators G_1-G_3 is 1.0 pu with no phase shift and G_4 and G_5 voltage is 0.98 pu with 10^o phase shift. The series inductive reactance is 2.73% pu. The coupled pi-section inductive reactance is 5.79% pu, the susceptance is 5.62% pu, and resistance is 1.89% pu. All the VSCs are identical, the base voltage (line-to-neutral) is 50.25 kV, the power is 100MVA, C=0.25F, the leakage reactance is 10.52% pu. The series coupling transformer has 30.32 MVA with leakage reactance is 1.0% pu, and has a winding ratio of 22.73 kV/9.21 kV.

The real and reactive power flow of line-2 is studied with unit-step changes. The reference is set as 2.4 pu and DC link voltage is 1.2 kV on line-1. The dynamic performance of real power flow of line-2 is shown in fig. 4. Although the optimized parameters are used, large fluctuations are present in the real power flow at t=1.5, 2.5 and 3.5 seconds. The API provides better performance than PI controller and it has fewer oscillations. As a result less overshoot characteristics. Fig. 5 shows the performance of reactive power flow of both the PI and API with unit-step changes in real power flow. From fig.5 one can easily understand that the performance of API controller is superior to PI controller. From the result one can observe that API successfully minimizes the coupling effect between two control loops. The ISE and IAE values are calculated for (0.9 < t < 5s) and is presented in table 2.

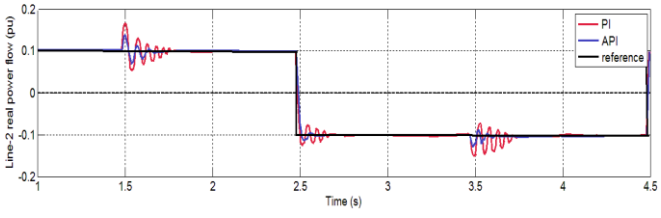

Figure 4. Dynamic performance of real power flow controller for master VSC.

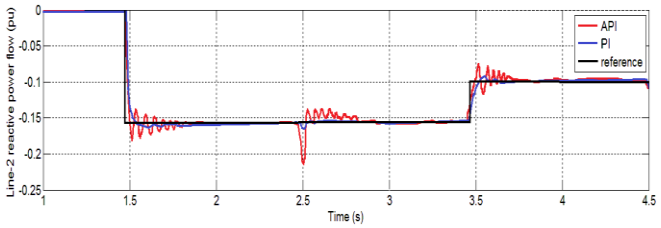

Figure 5. Dynamic performance of reactive power flow controller for master VSC.

The R_L/X_L ratio is increased by 3-time and the performance of real and reactive power flow is shown in fig. 6 and 7 respectively. Both the real and reactive power flow control loops are interacts adversely and the API provides better performance than PI controller and it has fewer oscillations as a result less overshoot characteristics. The proposed API minimizes the `interaction between both the control loops and gives a smoother response than PI. The ISE and IAE values are calculated for (0.9 < t < 5s) and the quantitative comparison is presented in table 2. In real power flow, the ISE is increased around 33.72% and the IAE is increased around 81% are computed for PI controller. Similarly, in reactive power flow, the ISE increased around 61.15% and the IAE is increased around 126.62% for PI controller. The dynamic performance of API controller is better and successfully reduces the interaction between both the real and reactive power flow.

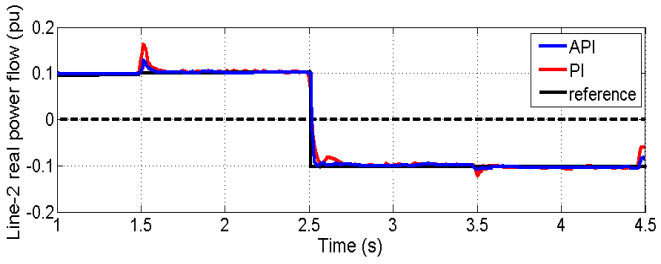

Figure 6. Dynamic performance of real power flow controller for master VSC (R_L/X_L>3 times of fig. 4)

Table 3. Overloaded lines and voltage violation buses before IPFC and IPFC with ADE and PSO techniques

Tripped Lines			Overloaded lines before IPFC				Overloaded lines after using IPFC							
							ADE after 100 trials				PSO Algorithm after 100 trials			
Line Number	From bus	To bus	From bus	To bus	% of Over Loading	Voltage violation buses	From bus	To bus	% of Over Loading	Voltage violation buses	From bus	To bus	% of Over Loading	Voltage violation buses
1	1	2	1 2 4	4 3 5	109.34 124.53 145.98	2, 3, 5, 6	2 4	3 5	108.12 113.83	-	2 4	3 5	105.03 115.35	-
4	2	4	1 3	2 5	127.31 134.69	1, 2, 4	1 3	2 5	101.92 105.72	-	1 3	2 5	103.94 107.83	-
2	1	3	2 3	3 4	142.39 128.72	1, 3, 4	3	4	109.24	-	3	4	114.39	-
7	4	5	-	-	-	3	-	-	-	-	-	-	-	-
8	5	6	1 2 5	3 6 6	142.85 129.45 119.54	1, 2, 5, 6	1 5	3 6	110.79 -	-	1 5	3 6	111.38 -	-
5	3	5	-	-	-	3, 4	-	-	-	-	-	-		-
9	3	4	2 4	5 5	143.87 138.82	2, 3, 5, 6	4	5	101.63	-	4	5	-	-

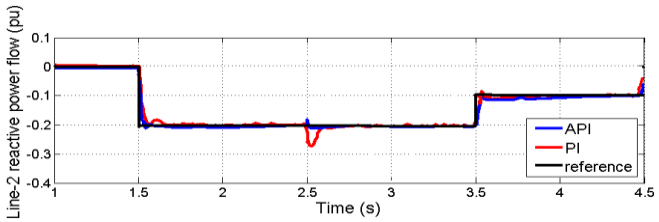

Figure 7. Dynamic performance of reactive power flow controller for master VSC (R_L/X_L>3 times of fig. 5)

The voltage limit range of 0.9-1.1 P.U is considered for determining voltage violation and 100% loading is considered for determining overloaded lines. Based on these considerations 7 lines comes under emergency scenario and the techniques ADE and PSO are applied to determine the voltage violation and overload lines. The ADE and PSO techniques are applied to the lines where the voltage violation and overloaded occurred. The bus voltage limit violations and overloaded lines with percentage of overloading before utilizing the IPFC and after IPFC with ADE and PSO techniques are presented in table 3. The results are obtained for 100 trials of each algorithm. From table 3 one can observe that the overloading of two emergency scenarios has been eliminated completely with the utilization of IPFC in the estimated location.

Table 2. Quantitative performance analysis of PI and API (IEEE 30-bus)

Case 1(IEEE 30-bus)				Case 2(IEEE 30-bus)			
Control Action	Controller	IAE	ISE	Control Action	Controller	IAE	ISE
Real power flow (line-2)	PI API	146.2033 89.5382	6.4312 4.4782	Real power flow (line-2)	PI API	153.4926 114.1836	6.5172 5.3812
Reactive power flow (line-2)	PI API	173.4824 74.8537	5.2847 3.1835	Reactive power flow (line-2)	PI API	172.2934 69.3952	5.6428 3.3851

The remaining five emergency scenarios did not eliminate the overloaded lines including IPFC in the optimized location. Even though, the power flows in these five contingencies are reduced considerably. Before inserting the IPFC in the optimal location, the percentage of overloading of some lines is very high which leads to trip the line and continuous failure will occur. After utilizing IPFC in the optimal location, voltage violations are eliminated but few of them are reduced with considerable amount of overloading. The optimal location of IPFC using ADE and PSO after 100 trials is shown in table 4.

There are five voltage violation buses before utilizing IPFC, and all the voltage violations are eliminated after utilizing IPFC. The congestion cost value of both the ADE and PSO after 100 trials is illustrated in fig. 8. From fig. 8 one can easily understand that the congestion cost value is lesser than PSO technique. On comparing the cost value of ADE with PSO it is around 14.5% lesser than PSO technique.

Table 4. Optimal location finding and real power generation after congestion management in IEEE 30-bus system.

Tripped Lines			Optimal location and Congestion Management			
			Optimal location		Real power after congestion management (MW)	
Line Number	From bus	To bus	ADE	PSO	ADE	PSO [25]
1	1	2	4	4	226.36	227.03
4	2	4	6	6	193.72	193.98
2	1	3	9	7	94.43	93.94
7	4	5	8	8	176.83	175.39
8	5	6	2	2	132.98	135.42
5	3	5	5	6	129.56	129.43
9	3	4	3	3	84.87	83.02

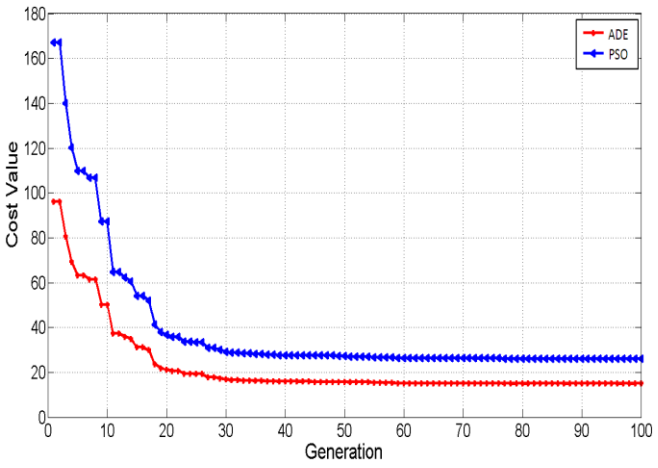

Figure 8. Congestion cost value of CSA and PSO techniques for IEEE 30-bus system

B. EEE 57-bus Test System

This system has 57-bus, 67 transmission lines, 8 generators, and 14 loads with 17 possible contingencies. The base voltage (line-to-line) is 160 kV and power is 100 MVA. The generators G_1-G_4 is 1.0 pu with no phase shift and G_5-G_8 voltage is 0.94 pu with 10^o phase shift. The series inductive reactance is 2.93% pu. The series coupling transformer has 34.72 MVA with leakage reactance is 1.0% pu, and has a winding ratio of 24.82 kV/11.36 kV. All the VSCs are identical, the base voltage (line-to-neutral) is 56.82 kV, the power is 110MVA, C=0.28F, the leakage reactance is 9.73% pu. The coupled pi-section inductive reactance is 6.24% pu, the susceptance is 5.84% pu, and resistance is 2.36% pu.

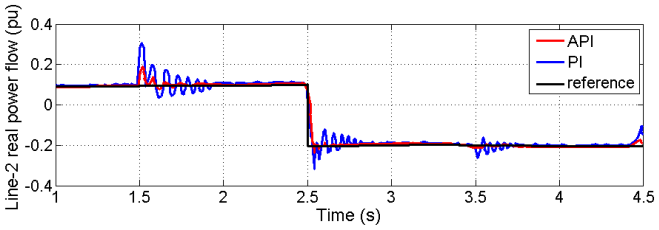

Figure 9. Dynamic performance of real power flow controller for master VSC.

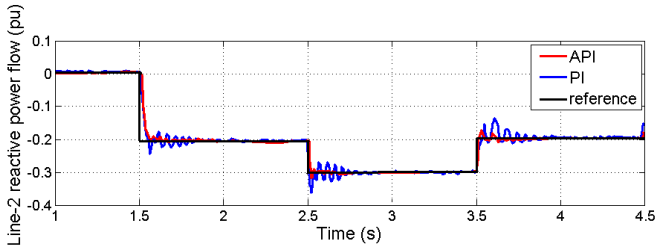

Figure 10. Dynamic performance of reactive power flow controller for master VSC.

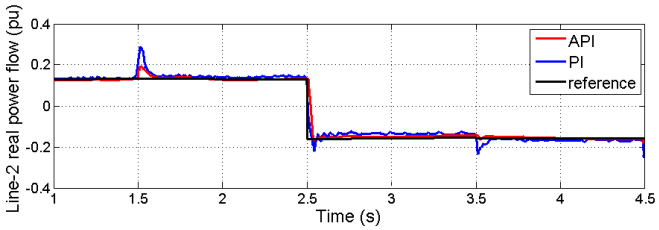

Figure 11. Dynamic performance of real power flow controller for master VSC (R_L/X_L>3 times of fig 9).

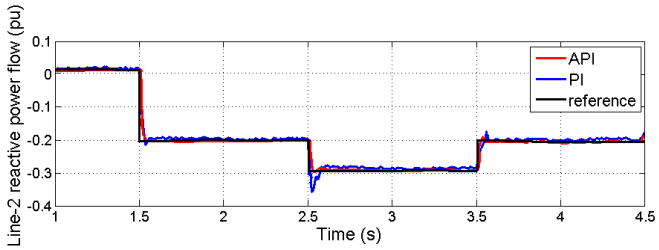

Figure 12. Dynamic performance of reactive power flow controller for master VSC (R_L/X_L>3 times of fig 10).

The real and reactive power flow of line-2 is studied with unit-step changes. The reference is set as 2.4 pu and DC link voltage is 1.2 kV on line-1. The dynamic performance of line-2in-terms of real and reactive power flow is shown in fig. 9. Large fluctuations are occurred at t=1.5, 2.5 3.5 and 4.5 seconds. The API has fewer oscillations and leads lesser overshoot characteristics compared to PI controller. Fig. 10 shows the performance of reactive power flow of both the PI and API with unit-step changes in real power flow for IEEE 57-bus system. From fig.10 one can observe that the performance of API controller is superior to PI controller. The result shows that API successfully minimizes the coupling

effect between two control loops. The ISE and IAE values are calculated for (0.9 < t < 5s) and is presented in table 5.

Table 5. Quantitative performance analysis of PI and API (IEEE 57-bus).

Case 1(IEEE 57-bus)				Case 2(IEEE 57-bus)			
Control Action	Controller	IAE	ISE	Control Action	Controller	IAE	ISE
Real power flow (line-2)	PI API	154.7354 89.8352	6.9533 4.7293	Real power flow (line-2)	PI API	159.7246 115.8532	6.7427 5.4932
Reactive power flow (line-2)	PI API	174.8522 73.4527	5.6235 3.2741	Reactive power flow (line-2)	PI API	176.8426 68.5912	5.8537 3.8429

Table 6. Overloaded lines and voltage violation buses before IPFC and IPFC with ADE and PSO techniques.

Tripped Lines			Overloaded lines before using IPFC				Overloaded lines after using IPFC							
			From bus	To bus	% of Over Loading	Voltage violation buses	ADE after 100 trials				PSO Algorithm after 100 trials			
Line Number	From bus	To bus					From Bus	To bus	% of Over Loading	Voltage violation buses	From bus	To bus	% of Over Loading	Voltage violation buses
1	1	2	1 2 6 8	4 3 7 9	102.35 164.43 143.64 121.43	3, 4, 6, 7	2 4	3 5	107.56 102.84	-	1 4	2 5	103.84 104.24	-
4	2	3	1 3 8	2 5 9	135.75 120.65 116.53	2, 4, 5, 9	5	6	110.40	-	5	6	113.92	-
7	4	5	2	4	129.62	4, 6				-			-	-
10	2	4	5	7	128.64	6, 8, 12	6	7	102.96	-	-	-	-	-
2	4	7	2	3	137.81	4, 8, 13	8	9	106.86	-	8	9	110.26	-
5	4	8	-	-	-	7				-				-
6	2	5	-	-	-	5				-				-
15	9	10	12	13	157.32	10, 14	12	13	116.93	-	12	13	101.56	-
17	5	6	2	4	142.62	4, 7, 10				-				-
8	6	12	-	-	-	11				-				-
9	3	7	-	-	-	14				-				-
11	8	13	-	-	-	14				-				-
14	10	14	10	12	128.45	12, 14	11	12	107.46	-	11	12	112.03	-
3	7	9	4	6	138.75	5, 6				-				-
18	11	13	10	12	123.74	14	13	14	104.26	-	13	14	109.19	-
12	12	14	7	11	133.81	8,10	-	-	-	-	-	-	-	-
20	13	14	3	8	127.30	-	-	-	-	-	-	-	-	-

The R_L/X_L ratio is set 3-times greater and the real and reactive power flow is shown in fig. 11 and 12 respectively. The proposed API minimizes the `interaction between both the control loops and gives a smoother response than PI. The ISE and IAE values are calculated for (0.9 < t < 5s) and the quantitative comparison of both the controller is presented in table 5. According to real power flow, the ISE is increased around 35.28% and the IAE is increased around 82.84% are computed for PI controller. Similarly, in reactive power flow, the ISE increased around 63.02% and the IAE is increased around 127.37% for PI controller. The dynamic performance of API controller is better and successfully reduces the interaction between both the real and reactive power flow.

The ADE and PSO techniques are applied to the lines where the controlling and congestion management is needed. The bus voltage limit violations and overloaded lines with percentage of overloading before and after utilizing the IPFC and after applying the algorithms ADE and PSO are presented in table 6. The results are obtained for 100 trials of each algorithm. From table 6 one can observe that eleven emergency scenarios have been eliminated completely by finding the location with the utilization of IPFC.

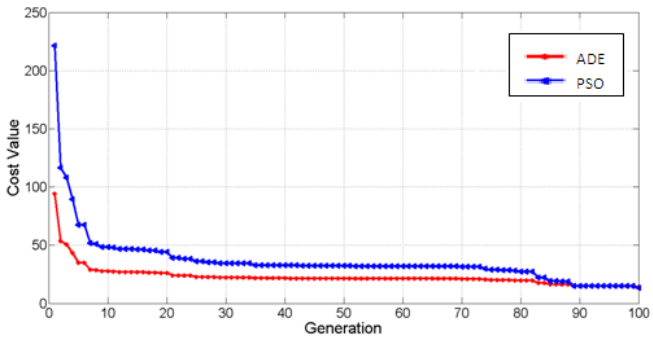

Figure 13. Convergence characterization of congestion cost value by ADE and PSO techniques for IEE-57 bus system.

After utilizing IPFC voltage violations are eliminated and most of the overloaded lines are eliminated but few of them are reducing the considerable amount of overloading and further correction function can be applied. The optimal location of IPFC using ADE and PSO with 100 trials is shown in table 7. The eight buses have voltage limit violation before and after utilizing IPFC and all the violations are eliminated. Fig. 13 shows the convergence characterization of both the ADE and PSO after 100 trials.The ADE and PSO techniques are applied to the lines where the controlling and congestion management is needed. The bus voltage limit violations and overloaded lines with percentage of overloading before and after utilizing the IPFC and after applying the algorithms ADE and PSO are presented in table 7. The results are obtained for 100 trials of each algorithm. From table 7 one can observe that eleven emergency scenarios have been eliminated completely by finding the location with the utilization of IPFC.

The remaining eight emergency scenarios did not eliminate the overloaded lines including IPFC in the optimized location. Even though, the flow in the eight contingencies is reduced. Before inserting IPFC the percentage of overloading of some lines is very high which lead to trip the line and continuous failure will occur. After utilizing IPFC voltage violations are eliminated and most of the overloaded lines are eliminated but few of them are reducing the considerable amount of overloading and further correction function can be applied. Fig. 13 shows the convergence characterization of both the ADE and PSO after 100 trials. The cost value of ADE is lesser than PSO around 12%. The congestion is created by increasing the demand of load and the simulated values of real power for different generators before and after congestion management using ADE are compared with PSO [25]. Comparison of congestion management cost for both the ADE and PSO techniques has been illustrated in fig. 14. The proposed ADE technique gives less congestion management cost than PSO.

Comparison of power loss before and after congestion management by using both the ADE and PSO technique is illustrated in fig. 15. From fig. 15 one can easily observe the power loss of the proposed technique is around 7% lesser than that of PSO. So the proposed ADE technique reduces the transmission congestion efficiently.

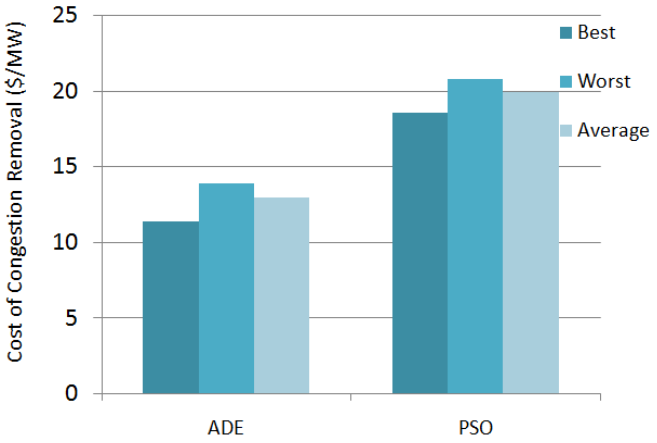

Figure 14. Comparison of cost of congestion removal in ADE and PSO.

Table 7. Real power generation before and after congestion management in IEEE 57-bus system.

Tripped Lines			Optimal location and Congestion Management			
			Optimal location of IPFC		Real power after congestion management (MW)	
Line Number	From Bus	To Bus	ADE	PSO	ADE	PSO [25]
1	1	2	2	2	243.86	260.73
4	2	3	4	4	183.53	184.63
7	4	5	7	7	276.76	275.73
10	2	4	1	1	186.43	185.43
2	4	7	4	4	287.43	286.23
5	4	8	3	3	196.34	195.23
6	2	5	10	10	143.86	644.10
15	9	10	5	5	97.34	97.01
17	5	6	11	11	243.82	240.92
8	6	12	3	3	125.95	123.89
9	3	7	8	8	169.52	168.83
11	8	13	9	9	284.83	284.53
14	10	14	12	12	194.52	190.91
3	7	9	14	14	93.29	90.23
18	11	13	7	7	83.73	81.73
12	12	14	11	11	142.32	140.03
20	13	14	12	12	123.83	119.23

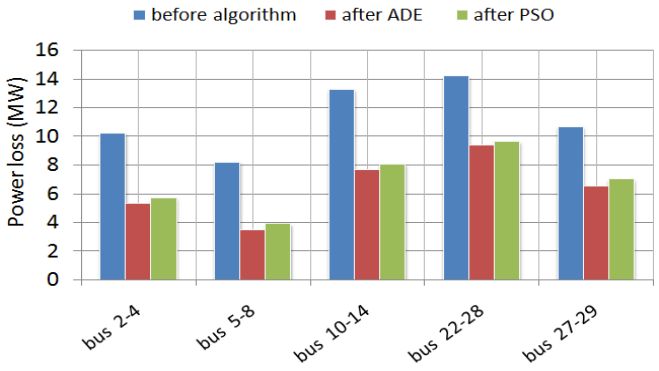

Figure 15. Power loss of ADE and PSO before and after congestion management.

6. Conclusion

In this paper, a new control scheme is proposed using adaptive PI controller for real and reactive flow control. The API is tested for both the IEEE 30-bus and IEEE 57-bus systems. Moreover the controller does not disturb other IPFC flow control and the dc link voltage control. The optimal location of IPFC and transmission congestion removal is done by using CSA and PSO has been investigated for improving the security of power system. Most severe emergency scenario has been analyzed and the priority allotted is based on the severity of the line. The new approach, CSA has been applied and the performance is compared with the PSO technique. The test performance for optimal location and congestion management were conducted for two test cases vice, IEEE 30-bus system and IEEE 57-bus system. The obtained results show that the CSA technique provides good computational efficiency, less cost of congestion removal, low power loss, stable convergence characteristics, and high quality solutions. Finally, the proposed method is used to determine the optimal location of IPFC, remove the congestion effectively and leads to increase the security of power system.

References

[1] Hingorani, NG., Gyugyi L. 2000, "Understanding FACTS: concepts and technology of flexible AC transmission systems", New York: Wiley IEEE Press. 2000.

[2] Singh, SN., Erlich, I, 2005, "Locating unified power flow controller for enhancing power system loadability", *In: International conference on future power system, Amsterdam*, Netherlands, Pp.162–66.

[3] Galiana GD et al, 1996, " Assessment and control of the impact of FACTS devices on power system performance." *IEEE Trans Power System*, 11(4), pp.1931–36.

[4] Chao Duan, Wanliang Fang, Lin Jiang, and Shuanbao Niu, 2015, "FACTS Devices Allocation via Sparse Optimization", *IEEE Transactions on Power Systems*, pp.1-15.

[5] Sheng-Huei Lee, Jiang-Hong Liu and Chia-Chi Chu, 2012, "Modeling and locating unified power-flow

controllers for static voltage stability enhancements", *International Transactions on Electrical Energy Systems*, 24(11), pp.1524-1540.

[6] Valentin Azbe, and Mihalic, 2008, "The Control Strategy for an IPFC Based on the Energy Function", *IEEE Transactions on Power Systems*. 23(4), pp.1662-1669.

[7] Gholipour, E., Isazadeh, b, 2013, "Design of a New Adaptive Optimal Wide Area IPFC Damping Controller in Iran Transmission Network", *Electrical Power and Energy Systems*, 53, pp.529-539.

[8] Vedik Basetti, Ashwani K. Chandel, 2015, "Hybrid power system state estimation using Taguchi differential evolution algorithm", *IET Science, Measurement & Technology*, 9(4), pp.449–466.

[9] Cai, H. R., Chung, C. Y., Wong, K. P, 2008, "Application of Differential Evolution Algorithm for Transient Stability Constrained Optimal Power Flow", *IEEE Transactions on Power System*, 3(2), pp.719-722.

[10] Guang Y Yang., Zhao Yang Dong., and Kit Po Wong, 2008, "A Modified Differential Evolution Algorithm with Fitness Sharing for Power System Planning", *IEEE Transactions on Power Systems*, 23(2), pp.514-522.

[11] Puja Dash., Lalit Chandra Saikia., Nidul Sinha, 2015, "Comparison of performances of several FACTS devices using Cuckoo search algorithm optimized 2DOF controllers in multi-area AGC", *Electrical Power and Energy Systems*, 65, pp.316-324.

[12] Taher Niknam., Mohammad Rasoul Narimani., and Masoud Jabbari, 2012, "Dynamic optimal power flow using hybrid particle swarm optimization and simulated annealing", *European Transactions on Electrical Power*, 23(7), pp.975-1001.

[13] Vijay Kumar, B., Srikanth, N.V, 2015, "Optimal location and sizing of Unified Power Flow Controller (UPFC) to improve dynamic stability: A hybrid technique. Electrical Power and Energy Systems", *Electrical Power and Energy Systems*, 64, pp.429–438.

[14] Hajforoosh, S., Nabavi, S.M.H., Masoum, M.A.S., 2012, "Coordinated aggregated-based particle swarm optimization algorithm for congestion management in restructured power market by placement and sizing of unified power flow controller", *IET Science, Measurement and Technology*, 6(4), pp.267–278.

[15] Sanjay Saini, Dayang Rohaya, B., Awang Rambli,, M.. Nordin, B., Zakaria, and Suziah B Sulaiman, 2014, "A Review on Particle Swarm Optimization Algorithm and Its Variants to Human Motion Tracking", *Hindawi Publishing Corporation. Mathematical Problems in Engineering, pp.*1-16.

[16] Zhang., Y., and Chen, C, 2006, "A novel power injection model of IPFC for power flow analysis inclusive of practical constraints", *IEEE Transactions on Power Systems*, 21, pp.1550-1556.

[17] Wang SK, Chiou JP, Liu CW, 2009, "Parameter tuning of power system stabilizers using improved ant direction hybrid differential evolution", *Int. J Electrical Power and Energy Systems*, 31, pp.34-42.

[18] Radu, D., Besabger, Y., 2005, "Blackout prevention by optimal insertion of FACTs devices in power system," In: Proc *IEEE future power system conference*.

[19] Storn, R., Price, K, 1997, "Differential evolution-a simple and efficient heuristic for global optimization over continuous spaces", *J Global Optimization*,11, pp.341-59.

[20] Price, KV, 1999, "An introduction to differential evolution", In: Corne D, Dorigo M, Glover M, editor. *New ideas in optimization*. London: McGraw-Hill, pp.79-108.

[21] Bernabe, S., Sanchez, A., Plaza, S., Lopez, J., Benediktsson, A., and Sarmiento, R, 2013, "Hyper spectral unmixing on GPUs and multi-core proces-sors: A comparison. IEEE J. Sel. Topics Appl. Earth Observ. Remote Sens, 6(3), pp.1386–1398.

[22] IEEE 30-bus and IEEE 57-bus test systems. available online: www.ee.washington.edu/research/pstca

[23] Wu, QH., Cao, YJ., Wen, JY, 1998, "Optimal reactive power dispatch using an adaptive genetic algorithm," *Electric Power Energy System*, 20, pp.563-569.

[24] Pinar Civicioglu, and Erkan Besdok, 2011, "A conceptual comparison of the Cuckoo-search, particle swarm optimization, differential evolution and artificial bee colony algorithms", *Artif Intell. Rev. Springer Science+Business Media B.V.*

[25] Milan Tuba, Milos Subotic, Nadezda Stanarevic, 2012, "Performance of a Modified Cuckoo Search Algorithm for Unconstrained Optimization Problems", *WSEAS Transactions on Systems*, 11, pp.62-73.

[26] Eberhart, RC., Kennedy, J., Shi, Y, 2001, Swam Intelligence. *San Francisco*: *Morgan Kaufman Publishers*. pp.61-284.

[27] Eberhart, RC., Shi, Y, 2001, "Particle Swam Optimization: development, applications and resources*", IEEE Press*, pp.90-283.

[28] Liu Yijian, He Xiongxiong, 2005, "Modeling identification of power plant thermal process based on PSO algorithm", *In: Proc American Control Conference*, 7, p.4484-4489.

Biographies

Dr.S.Arul received B.E (EIE), M.E (ECE) and Doctorate degree in the year 1992,2007and 2014 respectively. He is having 13 years of teaching experience and 7 years of industries. His areas of interests are Embedded Systems, computer network, control and instrumentation. He has published many papers in International / National Conferences and Journals He is currently working as an Associate Professor in the ECE department, Jeppiaar Institute of Technology affiliated by Anna University Chennai.